

UCSF

UC San Francisco Electronic Theses and Dissertations

Title

Identification of an Enamelin Defect Resulting in Amelogenesis Imperfecta

Permalink

<https://escholarship.org/uc/item/2jt9c41c>

Author

Massie, Jessica Claire

Publication Date

2011

Peer reviewed|Thesis/dissertation

Identification of an Enamelin Defect Resulting in Amelogenesis Imperfecta

by

Jessica Claire Massie

THESIS

Submitted in partial satisfaction of the requirement for the degree of

MASTER OF SCIENCE

in

Oral and Craniofacial Sciences

in the

GRADUATE DIVISION

of the

UNIVERSITY OF CALIFORNIA, SAN FRANCISCO

Identification of an Enamelin Defect Resulting in Amelogenesis Imperfecta

Jessica Claire Massie

ABSTRACT

Purpose: The purpose of this study was to identify the genetic defect in a child, which resulted in Amelogenesis Imperfecta (AI) using saliva collected from a routine patient visit.

Methods: A 10-year old female presented to the UCSF Pediatric Dental Clinic with sensitivity and esthetic concerns. She and her 59-year old father, both indicated a history significant for AI. Saliva was collected from the proband, her affected father, and her unaffected mother using the Oragene DNA collection kit from which their DNA was manually purified. A family history was taken to identify the mode of inheritance and enamelins (ENAM) was chosen as a candidate gene. Primer sets were generated to amplify the entire ENAM gene, and amplified products were sequenced.

Results: The family pedigree revealed an autosomal dominant inheritance pattern for AI. A clinical exam revealed a mixed dentition with generalized rough, pitted, yellow-brown enamel consistent with the hypoplastic phenotype reported for AI resulting from a defect in the enamel matrix protein, enamelins. PCR amplification of genomic DNA revealed a novel mutation in exon 7, at g.10602C>G that replaces Pro with Arg, which would alter the protein structure.

Conclusion: When patients present with inherited tooth defects, the dentist's role is to describe the phenotype and obtain a family pedigree of the inheritance pattern. Additionally, collecting a patient's saliva is a simple, painless procedure, which can be used for DNA purification, mutational analysis, and diagnosis of inherited tooth defects such as AI.

<u>TABLE OF CONTENTS:</u>	Page #
TITLE PAGE	ii
ABSTRACT	iii
TABLE OF CONTENTS	iv
1. INTRODUCTION	1
2. LITERATURE REVIEW	1
2.1. An Overview of Dental Development	1
2.2. Biology of Enamel Matrix and Enamel Formation	2
2.3. Genes Involved in Amelogenesis Imperfecta	3
2.3.1. X Chromosome-linked AI	3
2.3.2. Autosomal Inherited AI	5
3. CLASSIFICATION OF AI: PAST, PRESENT, AND FUTURE	11
3.1. Witkop's Classification of AI	11
3.2. The Modern Classification of AI	13
3.3. The Candidate Gene Strategy	14
4. PURPOSE	16
5. HYPOTHESIS	17
6. MATERIALS AND METHODS	17
6.1. General Study Design	17
6.2. Subject Selection	17
6.3. Dental Examination	17
6.4. Familial Inheritance	19

6.5. Saliva Samples	20
6.6. Polymerase Chain Reaction	21
6.7. Sequence Analysis	25
7. RESULTS	25
7.1. PCR and Sequencing	25
7.2. Mutational Analysis	27
8. DISCUSSION	30
8.1. The Role of the Dentist in Diagnosing and Treating AI	30
8.2. Photo Database of Previously Published AI Mutations	30
8.3. Novel Algorithm for Clinicians	32
8.4. Applying the Algorithm to the Family Studied	33
9. CONCLUSION	35
10. ACKNOWLEDGEMENTS	37
11. APPENDIX: Photo Database of Published AI Mutations	38
12. REFERENCE	43
13. UCSF Library Release Form	46

1. **Introduction**

Tooth enamel is an epithelial derived hard tissue covering the crowns of both the deciduous and succedaneous teeth. It is the *most* mineralized structure in the human body and is composed almost entirely of highly organized hydroxyapatite crystals. The entire process of enamel formation (amelogenesis) is under genetic control and is regulated by an expression of multiple genes. Disease causing mutations in the genes essential to enamel formation cause genetic tooth related defects, such as Amelogenesis Imperfecta (AI). AI refers to a diverse group of inherited enamel disorders, absent of systemic manifestations that are caused by mutations in a variety of genes encoding for enamel matrix proteins. Depending on the diagnostic criteria used and the demographics of the population studied, the prevalence of AI varies from 1:700 to 1:14,000.¹

2. **Literature Review**

2.1. An Overview of Dental Development

Teeth form as a product of interactions between the oral enamel epithelium and neural crest-derived ectomesenchyme². The dental lamina begins development at 6 weeks of embryonic age and differentiates from the basal layer of the oral epithelium. The dental lamina gives rise to the tooth bud, which further contains the enamel organ, dental papilla, and dental sac. The first stage of dental development is deemed the bud stage as the dental lamina begins to swell and undergo proliferation and morphodifferentiation. It is within the second, or cap stage of tooth development that the inner (concavity) and outer (convexity) form the enamel epithelium. The cap stage of development is

characterized by proliferation, histodifferentiation, and morphodifferentiation. Histodifferentiation encompasses the demarcation of odontoblasts (dentin) and ameloblasts (enamel). Anomalies of dental structure may occur when histodifferentiation is disturbed and the result may be Amelogenesis Imperfecta, Dentinogenesis Imperfecta (DI), or Osteogenesis Imperfecta (OI). Enamel apposition takes place in two stages: 1) partial mineralization as matrix segments are formed and 2) gradual completion of the matrix from the DEJ outward. Disturbances in enamel apposition leads to anomalies of *mineralized* enamel and dentin and may also cause forms of AI, DI, or OI.

2.2. Biology of Enamel Matrix and Enamel Formation

Dental enamel is formed within a distinctive extracellular matrix derived through the formation and secretion of proteins made by ameloblasts from the inner enamel epithelium³. Differentiating ameloblasts express small amounts of enamel proteins and as the basal lamina starts to break up, ameloblasts send cytoplasmic projections through the fragments. As the dentin starts to mineralize, surface ameloblasts project into the superficial collagen fibrils of the mantle dentin. Enamel matrix islands begin to appear along the irregular dentinal surface and enamel mineralization begins. The secretory ameloblasts start to recede and the islands of enamel grow and merge until an uninterrupted initial layer of enamel is deposited². This initial enamel layer is unorganized and aprismatic. It is when the secretory ameloblasts form extensions called Tome's processes, that the architectural basis for organizing enamel into rod and interrod is created². Ameloblasts secrete enamel proteins encompassing the crystals and into the space

previously occupied by the basal lamina creating a mineralization front. As the enamel crystals continue to grow in length and the ameloblasts continue their secretion of proteins, the mineralization front draws back with the Tome's process. The secretory stage results in longer enamel crystals and thicker enamel. Disturbances during this stage can cause enamel to be thin and hypoplastic. Illnesses or environmental effects on the developing enamel can lead to horizontal bands indicating the timing of disturbances during the secretory stage of enamel². As the ameloblasts continue to secrete proteins, the thickness of enamel continues to increase until the enamel layer is complete. Unfortunately, for every 1 in 700 to 1 in 14,000 person, a critical part of the fastidious process of amelogenesis is genetically mutated¹.

2.3. Genes Involved in Amelogenesis Imperfecta

There are thousands to possibly 10,000 genes involved in the formation of human enamel⁴. Autosomal dominant and recessive as well as dominant and recessive X-linked types of AI have been described. AI disorders are considered to be genetically heterogeneous and are thought to involve different mutations in the same or different genes^{1,5}. The regulation of these genes controls and dictates enamel formation. Mutations in some of the genes encoding specific enamel proteins have been found to cause Amelogenesis Imperfecta.

2.3.1. X chromosome-linked AI

Genetic linkage analyses carried out in families with X-linked AI have located mutations in the region Xp22.1-p22.3 corresponding to the

amelogenin (AMELX) locus. To date, 15 mutations in the gene encoding for the enamel protein, amelogenin (AMELX) have been found⁶.

Amelogenin is the most abundant of the enamel proteins and comprises approximately 80-90% of total enamel protein². In humans, the genes that code for amelogenin are located on the sex chromosomes: AMELX and AMELY, with only 10% of amelogenin being expressed from AMELY. Human amelogenin has a 16 amino acid signal peptide and typically contains 175 amino acids⁵. In general, amelogenin is necessary for orderly crystallite growth and spacing^{2, 5}. All of the X chromosome-linked AI cases (15) identified thus far are the result of mutations in the AMELX gene and cause either a hypoplastic or hypomaturational phenotype². The reason the phenotypes associated with the amelogenin gene are variable is mainly due to the fact that males and females are affected differently. In men, the general phenotypic description is that of a hypomature enamel that is yellowish, rough, and varies from a normal thickness to extremely thin or with local hypoplasia with neither prism structure nor retention of amelogenin type proteins. In females, the heterozygous phenotype has vertical bands of hypoplastic and normal enamel arranged linearly, with changes in color as a result of inactivation of one of the two copies of the X-chromosome, a phenomenon known as lyonization⁶.

2.3.2. Autosomal inherited AI

Theoretically, the other potential candidate genes involved in the autosomal inheritance of AI include tuftelin (TUFT), ameloblastin (AMBN), amelotin (AMTN), enamelin (ENAM), enamelysin (MMP-20), kalikryn 4 (KLK-4), distal-less 3 homeobox gene (DLX3), FAM83H, and the gene encoding the beta propeller WDR72. Currently, of these genes, ENAM, MMP20, KLK4, DLX3, FAM83H, and WDR72 are considered causal genes because mutations in their coding regions have been reported to cause AI. No mutations have been reported in the TUFT, AMBN, and AMTN genes, but they continue to be classified as candidate genes.

Tuftelin (TUFT) is an acidic glycoprotein found in tooth enamel. It was cloned and mapped to chromosome 1q.21-31 which is an autosomal chromosome. It has been suggested to play an important role during the development and mineralization of enamel. It has been proposed that TUFT acts to start the mineralization process of enamel and although it has yet to be discovered, is a legitimate candidate gene for AI^{7,8}.

Amelotin (AMBN) is a protein expressed and secreted by ameloblasts, but its distribution during enamel development is not yet clear. There is strong evidence to show that amelotin starts to secrete at a very early stage in enamel development and is transiently expressed throughout the process of enamel development. It is situated close to ameloblastin and enamelin on human chromosome 4. The expression of

amelotin is exclusively defined to dental tissues and the co-expression of amelotin, ameloblastin, amelogenin, and enamelin suggest that enamel biomineralization may be the result of a cooperative enamel protein effort. Amelotin continues to be a candidate gene for AI and additional studies are necessary to advance the knowledge of amelotin in enamel development⁹

Ameloblastin (AMBN) is an enamel matrix protein, which comprises roughly 5% of the total protein found in developing enamel². Human AMBN is composed of a 26 amino acid signal peptide and 421 amino acids. Throughout enamel formation, ameloblastin is generally lost soon after secretion, but a select few cleavage products are spatially distributed throughout the enamel. Ameloblastin is a fundamental protein in enamel of the enamel matrix of developing teeth¹⁰. Mice develop severe enamel hypoplasia in the homozygous negative condition (*Ambn*^{-/-})¹⁰. Human AMBN mutations have yet to be discovered, most likely because AMBN is normally secreted in ample quantities so that a reduction (haploinsufficiency) in its expression may not produce the phenotype. AMBN is still considered a candidate gene because AI as a result of a mutation in AMBN most likely follows an autosomal recessive pattern of inheritance and although rare, will likely be discovered one day even though its linkage to the disease is yet to be proven¹⁰.

Enamelysin (MMP-20) is a protease that is secreted during the early secretory stage of enamel formation during the lengthening of the

crystallites. The role of MMP-20 is to cleave the enamel proteins, which are then degraded. As the degradation of the proteins continues, space between the crystallites becomes available which allows for the thickening of crystals and a net replacement of protein by mineral¹¹. In the case of autosomal recessive AI, it is believed that defects in both MMP20 alleles causes a lack of thickening in the crystallite layer due to the failure of the MMP20 to progressively remove the enamel matrix proteins. Oftentimes this defect will cause enamel sheering under the forces of mastication¹¹.

Kalikryn 4 (KLK-4) is a protease, which can target the degradation of enamel proteins with great specificity. KLK-4 is thought to *aggressively* cleave residual enamel proteins as it is secreted at the stage just prior to the (precipitous) drop in matrix enamel proteins. As KLK-4 functions during the later stages of enamel formation to degrade enamel proteins and replace protein with mineral, patients with autosomal recessive AI carry defects in both KLK-4 alleles and as a result, the enamel is less highly mineralized, aberrantly soft, and oftentimes pigmented¹¹.

The DLX3 gene is a member of the family of homeobox genes that are homologous to the *distal-less* gene of *Drosophila*. Mutations in this gene cause tricho-dento-osseous syndrome (TDO), which is distinguished as enamel hypoplasia with coinciding root taurodontism, curly hair at birth, and a thickened, dense skull. In 2005, a paper was published demonstrating that a mutation within the DLX3 gene was associated with

amelogenesis imperfecta hypoplastic-hypomaturation with taurodontism (AIHHT) and that TDO and some forms of AIHHT are allelic¹². It is still under investigation as to whether or not TDO is somehow associated to AIHHT^{2, 12}.

Most recently, another gene known to cause AI was discovered. The FAM83H gene causes autosomal dominant hypocalcified AI (ADHCAI), which is the most common type of AI in North America. The role of the FAM83H gene in enamel formation remains unclear, but the gene is expressed in many other tissues. However, the only known mutations in the FAM83H gene result in enamel abnormalities, indicating that the gene is required for proper enamel calcification and possibly less important in other tissues throughout the body. The typical phenotype in patients with FAM83H mutations includes both sets of dentition appearing yellowish-brown with enamel that is prone to fracture. The enamel has a marked decrease in mineral and an increase in protein. There are currently 13 mutations published in FAM83H and this new genetic discovery is especially important in North America where most of the AI cases are classified as being ADHCAI⁴.

The gene encoding the beta propeller WDR72 has been reported to cause AI. The gene consists of 19 coding exons and is roughly 250kb in size. Although very little is known about the gene, we do know that its closest human homolog is WDR7 (Rabconnectin-3 β). Rabconnectin contributes to activation and deactivation of RAB3A, which is a GTP-

binding protein necessary for vesicle turnover, critical to maturing ameloblasts. The possibility that WDR72 functions similar to that of WDR7 and may also be important in Ca^{2+} vesicle turnover and maturing ameloblasts, provides an insight as to why and how WDR72 causes autosomal recessive AI¹³.

Enamelin is the largest and least abundant of the enamel matrix proteins however, it appears to be the most significant contributing factor in the etiology of autosomal dominant AI². It is a tooth-specific gene expressed primarily by ameloblasts¹². The earliest signal for enamel protein was seen in differentiating ameloblasts at the stage where the basal lamina started to break up. Just before the enamel signal disappears in early maturation, it extends from the DEJ to the Tomes' process, is particularly strong beneath the secretory end of the Tomes' process, and is scarce in the sheath space. This phenomenon is termed the "reverse honeycomb pattern" and suggests that enamel proteins and their products separate into different compartments and are not simply degraded but become functional polypeptides. The antibody specific for the N-terminus of the enamel cleavage product shows a concentration of signal that diminishes into the depth of the developing enamel, indicating that this portion of enamel is rapidly degraded and does not accumulate in the enamel matrix. On the other hand, the antibody specific for the C-terminus of the enamel cleavage product, which is only observed under the secretory end of the Tomes' process, in fact, is present at the

mineralization front and plays a role in the elongation of enamel crystals.

In summing up the role of enamelin, it is important to note that it functions only during dental enamel formation (ie. crystal elongation) and is expressed predominately by secretory ameloblasts¹⁴.

Presently, there are eight published reports of ENAM mutations causing ADAI and more recently, one family was reported as transmitting an ENAM caused by an autosomal recessive mode of inheritance. The phenotypes of localized hypoplastic (mild) and generalized thin hypoplastic (severe) are associated with ENAM mutations. Enamelin is normally expressed in the proper amount for enamel formation and when the quantity is reduced, due to haploinsufficiency, the localized hypoplastic phenotype is seen. When there is considerable mutation in ENAM and its subsequent protein, there is a generalized thinning of enamel caused by the failure of uncleaved enamelin to assist in crystal elongation¹⁵.

Only recently have the advances in mutational analysis using the candidate gene approach allowed researchers and clinicians to classify enamel defects by genotype. Carl J. Witkop was a pioneer in the field of human genetics and dental health and in 1956 at the age of 36 he became the chief of the Human Genetics Section at the NIDR. His professional accomplishments in the area of inherited tooth defects were the first comprehensive approach to the subject. In 1957, Witkop published a paper entitled *Hereditary Defects in Enamel and Dentin*, which classified

enamel defects primarily on phenotype. In 1971, Witkop and Rao published *Inherited Defects in Tooth Structure*, which further classified Amelogenesis Imperfecta by phenotype and secondarily, by mode of inheritance. The classification system established in 1971 by Witkop and Rao was further modified over the years following its introduction, but it was not until 1995 when Aldred and Crawford incorporated genetic analysis into the classification system.

3. **Classification of Amelogenesis Imperfecta: Past, Present, and Future**

3.1. **Witkop's Classification of AI**

Since 1945, classifications of Amelogenesis Imperfecta have evolved from a solely phenotype based system to a method that incorporates inheritance pattern and even more currently, molecular genetics. In 1971, CJ Witkop followed the clinician-centered classification system, which was popular in medicine at the time, and classified AI according to phenotype (hypoplastic, hypocalcified, or hypomaturation) and secondarily classified AI by the mode of inheritance. In the same paper, Witkop also defined AI as 'a group of disfiguring hereditary conditions' which 'affect the clinical appearance of enamel of all or nearly all the teeth, which occur in kindreds such that all the individuals in the kindred show essentially the same defect and which are unassociated with the known morphologic or biochemical changes elsewhere in the body'. Table 1 illustrates the classic AI classification system as proposed by Witkop and Rao in 1971.

Table 1. Classification of Amelogenesis Imperfecta¹⁶

1. Hypoplastic
 - a. Autosomal dominant hypoplastic-hypomaturation with taurodontism
 - i. Winter type
 - ii. Crawford type
 - b. Autosomal dominant smooth hypoplastic with eruption defect and resorption of teeth
 - c. Autosomal dominant rough hypoplastic
 - d. Autosomal dominant pitted hypoplastic
 - e. Autosomal dominant local hypoplastic
 - f. X-linked dominant rough hypoplastic
2. Hypocalcified
 - a. Autosomal dominant hypocalcified
3. Hypomaturation
 - a. X-linked recessive hypomaturation
 - b. Autosomal recessive pigmented hypomaturation
 - c. Snow-capped teeth, autosomal dominant
 - d. White hypomature spots?

Table 1 shows the 1971 Witkop classification of Amelogenesis Imperfecta. It is the “classic” identification system upon which many clinicians still rely

The progress made on AI classification between 1971 and the early eighties was inconsistent, confusing, and of questionable value at best. In 1988, the predominately phenotypic classification of Witkop was revised into four major types of AI (hypoplastic, hypomaturation, hypocalcified, and hypomaturation-hypocalcified) with 15 subtypes and a secondary basis of classification by mode of inheritance¹⁷. In the same year, Witkop and several others had realized his initial mistake in suggesting that ‘all the individuals in the kindred show essentially the same defect’. In fact, by this time previous efforts to classify AI according to clinical appearance had been overtaken by two key

occurrences: first, the known phenotypic variation *within* family pedigrees and secondly, the advances in the knowledge of the human genome¹⁷.

3.2. The Modern Classification of AI

Finally, in 1995 Aldred and Crawford attempted to make sense out of the years of classifying AI based on confusing clinical descriptions and proposed a classification system for AI based on the molecular defect, mode of inheritance, and lastly, phenotype. It was the unofficial commencement of the candidate gene based system of classification.

Currently, it is recognized that the advancement in dental genetics requires an AI classification model based upon genetic data in conjunction with mode of inheritance and phenotype as a secondary discriminator. AI can be transmitted by either an autosomal dominant, autosomal recessive, or X-linked mode of inheritance¹⁷. As the genetic background of AI is becoming more fully understood, mutations in (six) genes have been found to cause AI. As more mutations associated with various AI types are discovered we expect the ability to make accurate diagnoses to be greatly improved.

A study by Aldred et al in 2002 used molecular genetics to establish the mode of inheritance in a family with AI where it was unclear whether the AI was transmitted by autosomal dominance or X-linked dominance. A single base deletion mutation was identified in exon 6 of the amelogenin gene and confirms that the mode of inheritance was X-linked, which was critical for genetic counseling within this family. The study illustrates the essential role that genetic analysis plays in correctly identifying the mode of inheritance and AI diagnosis.¹⁸

Previous studies have well established the hereditary patterns and clinical phenotypes of AI allowing for a modern day focus on genetic etiology. Evaluating the clinical presentation and hereditary pattern via a detailed family pedigree can facilitate a prioritized list of candidate genes to sequence.¹⁹ The candidate-gene-based mutational analysis is currently the most appropriate and acceptable method for diagnosing AI according to the most recent literature.

3.3. The Candidate Gene Strategy

The candidate gene approach to diagnosing AI has evolved from decades of attempts to classify this disease. As reviewed previously, the traditional classification system utilized primarily phenotype with a secondary emphasis on inheritance pattern. As we continue focusing our efforts on the molecular genetic etiology of AI, a paradigm shift in the classification and diagnosis of AI remains inevitable.

To date, mutations in genes encoding all of the enamel matrix proteins (ENAM, AMELX, KLK4 and MMP20, DLX3, FAM83H, and WDR72) with the exception of ameloblastin (AMBN), amelotin (AMTN) and tuftelin (TUFT1) have been identified.¹⁹ These genes are therefore the primary candidates for non-syndromic hypoplastic and hypomatured AI. Mutations in FAM83H have been found to cause hypocalcified AI, which makes FAM83H the primary candidate gene in patients with non-syndromic, autosomal dominant, hypocalcified AI (ADHCAI).²⁰ Mutations in the DLX3 gene cause tricho-dento-osseous (TDO) syndrome, which is an autosomal dominant disorder named for the most commonly affected tissues: hair, teeth, and bones. The DLX3 gene is the primary

candidate gene in families where autosomal dominant AI is associated with the classic features of TDO syndrome (kinky or curly hair, taurodontism, and increased thickness and density of cranial bones).²¹

As described previously, Aldred and Crawford proposed the most recent AI classification to date in 1995. They included cataloguing AI based on mode of inheritance, molecular basis, biochemical outcome, and phenotype. Their proposition follows the principal idea that the primary structure for the classification of AI must be based not primarily on phenotype, but on mode of inheritance and genetic analysis. Their classification scheme was astute and progressive but provided no more than a catalogue of AI mutations and was therefore, not clinically relevant.

In 2009, Kang et al created a strategy diagram using a candidate gene-based mutational analysis of persons with AI. Again, an attempt was made to utilize a candidate gene approach but the diagram reverts back to phenotypic descriptors as the primary foundation on which the entire system is based.

Figure 1. Strategy diagram of candidate-gene-based mutational analysis¹⁹

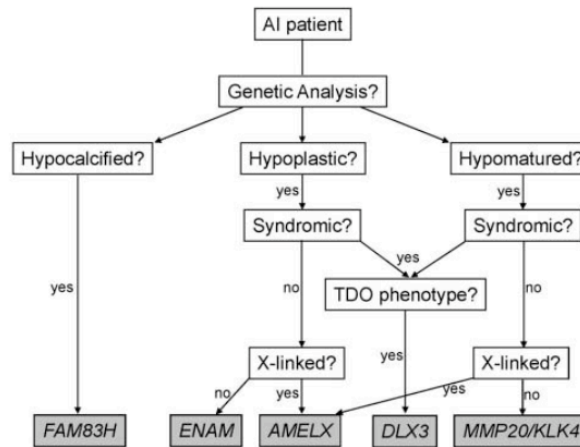


Figure 1 is a strategy diagram created by Kang et al in 2009, which is the first attempt at simplifying the candidate gene approach to diagnose of AI. Unfortunately it uses phenotype as the primary distinction between types of AI.

The diagram incorporates the three critical factors of inheritance pattern, genetic analysis, and phenotype, but it continues to put an undue emphasis on phenotypic characteristics. In addition, application of the previous attempts at classifying AI types is hampered by the interfamilial variability of the AI phenotype.²²

4. **Purpose**

The purpose of the present study was to utilize the candidate gene strategy to discover the genetic mutation causing one family's Amelogenesis Imperfecta. In addition, as the classification of AI transforms from one that is antiquated to a modern, genetic based system, this study intended to create a new strategy diagram, specifically designed with the clinician in mind for the purpose of making a diagnosis based on a candidate gene approach.

5. **Hypothesis**

In the *clinical* setting, saliva collection can be used as a screening tool enabling the practitioner to diagnose genetic tooth related defects (i.e. Amelogenesis Imperfecta).

6. **Materials and Methods**

6.1. General Study Design

The Committee on Human Research (CHR) at the University of California San Francisco (UCSF) approved this project as part of the Molecular Genetic Investigation in Patients with Congenital Anomalies study. The experiments were undertaken with the understanding and written consent of each person prior to

6.2. Subject Selection

The parents of a 10-year-old female patient from Bozeman, Montana sought treatment at UCSF for their daughter's Amelogenesis Imperfecta and provided consent for treatment and genetic analysis. Procedures, benefits, risks, and rights of the subjects were discussed with the subjects and the subject's parents. The patient gave her assent to participate in the study and the parents consented, allowing their daughter to be a participant in the study. The parents gave their written consent to participate as affected father and unaffected mother.

6.3. Dental Examination

The family sought restorative care for their daughter from UCSF pediatric dentistry. The child's chief complaint was that her teeth were sensitive and she did not like the way they looked. Her prenatal and medical history was

noncontributory. Her mother reported a pregnancy without complications. Clinical examination of the daughter revealed a mixed dentition. The patient claimed to have sensitivity to thermal stimuli while eating and drinking. The teeth appeared yellowish-brown, rough, and lacked proximal contacts. The enamel appeared irregular with areas of thin, rough enamel (Figure 3). All of the first permanent molars were erupted and exhibited Class I occlusion. The primary lower second molars and permanent upper first molars had already been restored with stainless steel crowns (SSCs). The soft tissue appeared pink and healthy as the patient had optimal oral hygiene. She had an overjet of 1mm (no anterior open bite) and an overbite of 50%. There was no evidence of taurodontism. After consulting with a Prosthodontist, a treatment plan was formulated to restore the upper anteriors with fiber reinforced composite crowns and the lower incisors with direct composite veneers to aid in preventing sensitivity, further enamel breakdown, and to improve esthetics.

Figure 3. Clinical Phenotypes of Subject

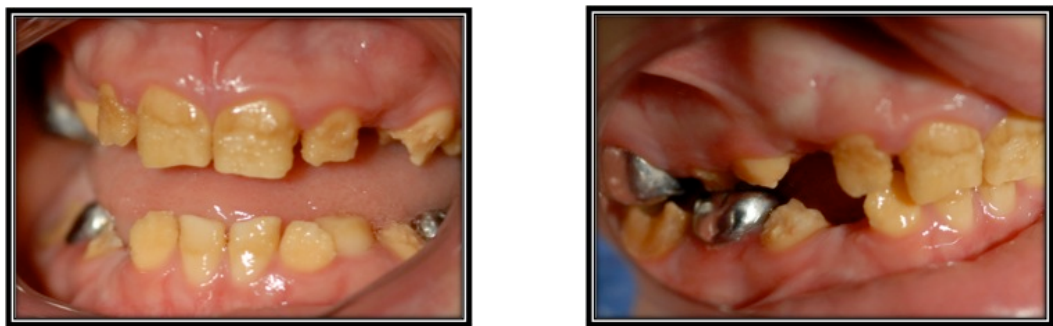


Figure 3 displays the frontal and lateral photos of our subject prior to restorative and esthetic treatment.

6.4. Familial Inheritance

Her father indicated a history significant for AI, as reported to him by his dentist, who had performed extensive dental rehabilitation for him over the years. The father also stated that his mother is 85 and lives in northern Spain where she has had “bad teeth” all of her life. The father also reported that 2 of his 3 brothers had been told that they have AI (Figure 4). The mother denied any history of AI. According to the reported family history, the inheritance pattern was determined to be either autosomal dominant or X-linked dominant.

Figure 4. Pedigree of Subject and her Family

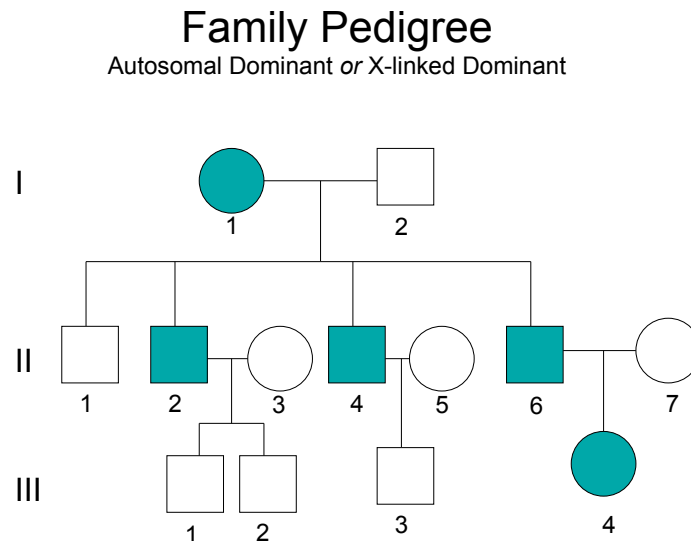


Figure 4 depicts the pedigree of the family in this study. The teal colored circles and squares represent affected individuals. This familial pattern appears to be of dominant (x-linked or autosomal) inheritance.

6.5. Saliva Samples

The research study was explained to the family and after complete review of the informed consent and the patient's Bill of Rights, the subjects signed separate informed consents. A 12-17 year old specific assent was reviewed with the minor. Saliva samples were collected from the patient and her parents for mutational analysis. The samples were labeled III:4, II:6, and II:7 for identification purposes. Genomic DNA was isolated from saliva by means of the Oragene DNA collection kit (DNA Genotek, Ottawa, ON Canada). 2mL of saliva was collected from the patient, her mother, and father in separate Oragene OG-250 collection discs after being advised not to eat, drink, smoke, or chew gum for 30 minutes prior to the collection. After the saliva was collected, the lid was screwed on tight allowing each of the saliva samples to mix with the Oragene DNA solution, which stabilized the DNA.

The samples were transported to the lab where kept at room temperature until they underwent purification. The purification steps were closely followed per the manufacturers instructions (Table 1). Prior to the purification of the DNA in saliva, the equipment and reagents were collected. The equipment necessary for the purification steps included a microcentrifuge capable of running at 13,000 rpm and an air or water incubator at 50°. The reagents necessary included room temperature 100% ethanol, room temperature 70% ethanol, glycogen (20mg/mL), and a DNA buffer. The DNA buffer was mixed according to the formula described: TE (10mM Tris-HCl, 1mM EDTA, pH 8.0) and utilized in the purification steps when indicated.

Table 1. Laboratory Protocol for DNA Purification Using Oragene Kit

Purification Steps
1. Mix the Oragene DNA/saliva sample by inversion and gentle shaking for a few seconds
2. Incubate the sample at 50°C in a water incubator for a minimum of 1 hour
3. Transfer 500µL of the mixed Oragene DNA/saliva sample to a 1.5mL microcentrifuge tube
4. For 500µL of Oragene DNA/saliva, add 20µL of Oragene DNA Purifier (supplied by the Oragene kit) to the microcentrifuge tube and vortex for a few seconds
5. Incubate on ice for 10 minutes
6. Centrifuge at room temperature for 5 minutes at 13,000 rpm
7. Transfer the clear supernatant into a fresh microcentrifuge tube. Discard the pellet containing impurities
<i>Optional step: Addition of Glycogen (add 5µL of Glycogen to the supernatant to make the pellet more easily visible)</i>
8. To the 500µL of supernatant, add 500µL of room temperature 100% ethanol. Mix by inversion 10 times
9. Allow the samples to stand at room temperature for 10 minutes to allow the DNA to fully precipitate
10. Microcentrifuge the tube at room temperature for 2 minutes at 13,000 rpm
11. Remove the supernatant and discard it
12. Add 250µL of 70% ethanol. Let stand at room temperature for 1 minute. Completely remove the ethanol without disturbing the pellet
13. Add 100µL of DNA TE buffer to dissolve the DNA pellet. Vortex for 5 seconds
14. To ensure complete hydration of the DNA, incubate at room temperature for 1-2 days and store at 4°C for up to 1-2 months (Long term at -20°C)

Table 1 lists the Oragene protocol for purifying DNA from saliva samples. Each of the steps was followed to ensure that proper purification was achieved.

6.6. Polymerase Chain Reaction

After the DNA was purified and fully rehydrated, each of the three samples was run through the NanoDrop Spectrophotometer (Thermo Scientific, Wilmington, DE) to measure the purity and concentration of the DNA using the OD_{260}/OD_{280} ratio. The samples measured 298.1 ng/µL, 54.5 ng/µL, and 418.7 ng/µL for II:6, III:4, and II:7, respectively. Due to the difference in concentrations, the III:4 sample was amplified using a slightly different PCR

formulation (see below). Following the purification of DNA from the three samples, a mutational analysis of the ENAM gene was performed.

The ENAM gene is located on the long arm of chromosome 4 at position 13.3 and has 10 exons, two of which are non-coding (Figure 5). In the present study, exons 3 through 10 were amplified using PCR. Primers for each exon were chosen according to previous reports.²³⁻²⁵ For exons 3 and 8, the previously reported primers did not give us proper results and new primers were designed for this study. PCR amplifications were carried out for each of the ENAM exons as described in Table 2.

Figure 5. Human ENAM gene with range of amino acids encoding each exon

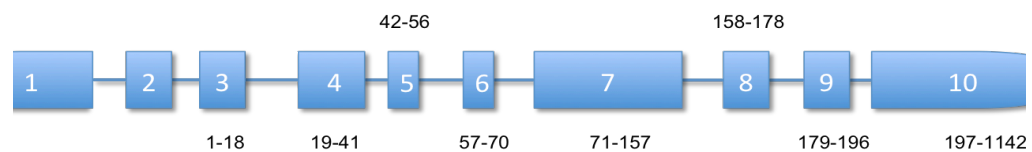


Figure 5 is an illustration of the enamel gene and depicts the exons (blocks) and introns (lines) as well as the size of each exon. Exon 1 and 2 are non-coding regions of the gene.

Table 2. Primers used to amplify ENAM

Exon	Sequence 5'–3'	Size (bp)	Annealing temp (°C)
3	F: TGCAACATCGCCCTAGAA	595	55
	R: GGATGACTGAGATCCCTTCC		
4–6	F: TAGATAAGTGCAGAGTGCCC	1,181	58
	R: GGTGTCTCTATTGACTAAGGC		
7	F: GAGACAGCCTGAATCACAGC	361	58
	R: CGAGGCCATTTACAGATATGG		
8	F: GATTGGAATCCTGGCTTCAG	552	61
	R: TGCCTGGTTTTGTTTCATACC		
9	F: AATGGCGGCATCGAACGTGG	155	56
	R: TGGATTGTAATTTCTAGTGGAG		
10a	F: AACACCATGGTGGGAAACAAAG	573	58
	R: TTACGTTCCAAGCAAAGAAGTTC		
10b	F: ACAGAATAGGCCTTTTACAGA	787	60
	R: ATATGGGTATATTCAGGGTAGAA		
10c	F: CAAGAAGAACATTTACCCCATCCT	753	60
	R: CATGCCATAGTTCAAATTCACCC		
10d	F: AGCTGGGCTTCAGAAAAATCCAAT	709	60
	R: AGATGGTCTTTGCTGTTGCCTCTC		
10e	F: CTCCAATCCAGAAGGCATCCAA	510	60
	R: CTCCACCTGGGTCGCTACTCCTAT		

Table 2 is the compilation of forward and reverse primers used in this project to amplify specific DNA sequences.

PCR was performed in a 25 μ L volume with the use of DNA Taq Polymerase (Invitrogen, Foster City, CA). PCR reactions were run with a positive (cDNA) and negative (water) control and each tube contained 2.5 μ L 10X PCR buffer, 0.75 μ L 50nM MgCl₂, 0.5 μ L 10mM dNTP, and 14.1 μ L dH₂O. In addition, 0.5 μ L of each forward and reverse primer, 2 μ L sample DNA (positive control: 2 μ L cDNA, negative control: 2 μ L water), 4 μ L water, and 0.15 μ L Taq polymerase were added to each tube. Due to the fact that the concentration of DNA in III:4's

saliva was much less than that of her parents, the specific formulation for the PCR run with her DNA included 0.5 μ L of each forward and reverse primer, 4 μ L sample DNA (positive control: 4 μ L cDNA, negative control: 4 μ L water), 2 μ L water, and 0.15 μ L Taq polymerase.

Amplification was performed in a GeneAmp 9700 thermal cycler (Applied Biosystems, city, state). After an initial incubation for 4 min at 94°C, samples were subjected to 35 cycles of 30 seconds at 94°C, then 1 minute at 55°C, and 1 minute at 72°C. Then the final extension step was performed at 72°C for 10 minutes.

After amplification of all exons, each sample (including the positive and negative controls) was mixed with 6X loading dye (BioLabs, Ipswich, MA). The sizes and quantities of the products were analyzed using a Quick-Load™100-bp DNA ladder (BioLabs, Ipswich, MA) loaded onto a 1.7% agarose gel stained with Sybr®-Green detection dye (Applied Biosystems, Foster City, CA).

Electrophoresis was performed with the conditions of 100V in TE buffer for 30-40 minutes in order to evaluate the reliability and success of the primer in amplifying the correct exon. Figure 6 is an actual gel that was run with II:6 10 a, b, c, and d with a 100-bp ladder indicating that the primers worked appropriately. Prior to sending out PCR products for sequencing, each of the products was run through gel electrophoresis for the purpose of ensuring that appropriate samples were being sent for sequencing.

6.7. Sequence Analysis

The concentrations of the samples were recorded using the NanoDrop Spectrophotometer (Thermo Scientific, Wilmington, DE). PCR products and correlating primers were sent to Elim Biopharmaceuticals (Hayward, CA) for sequencing. The samples were sent non pre-mixed with a concentration of $>10\text{ng}/\mu\text{L}$, and $> 10/\mu\text{L}$, per the instructions on their website. The lengths of the PCR products as well as the specific annealing temperatures for each primer were submitted. Primers were mixed to a concentration of $3\mu\text{M}$.

The sequencing data was received from ElimBio and uploaded into CodonAligner (CodonCode Corporation, Dedham, MA) for analysis. The chromatograms were analyzed using the CodonAligner software. The resulting sequences were assembled and compared with the wild-type NG_013024 from Genbank.

7. Results

7.1. PCR and Sequencing

Prior to sending out the PCR products for sequencing for each of the three individuals studied (II:6, III:4, and II:7), it was imperative to determine whether or not the primers worked. As described in the materials and methods section above, each sample run through PCR was subsequently run on a gel to determine the success of the primer. The Quick-LoadTM 100 bp DNA ladder serves as a guide from which to measure the size of each PCR product. In figure 6 below, the products for exon 10 run with II:6's DNA can be seen. This figure illustrates how

each of the PCR products were run after being amplified. Prior to sending the PCR products to sequencing, the gel were required to show that the primer worked as seen with the positive control, the negative control was in fact negative, and that the size of the PCR product matched up with the size of the exon sequence being amplified.

Figure 6. Gel of II:6 -10 a, b, c, & d

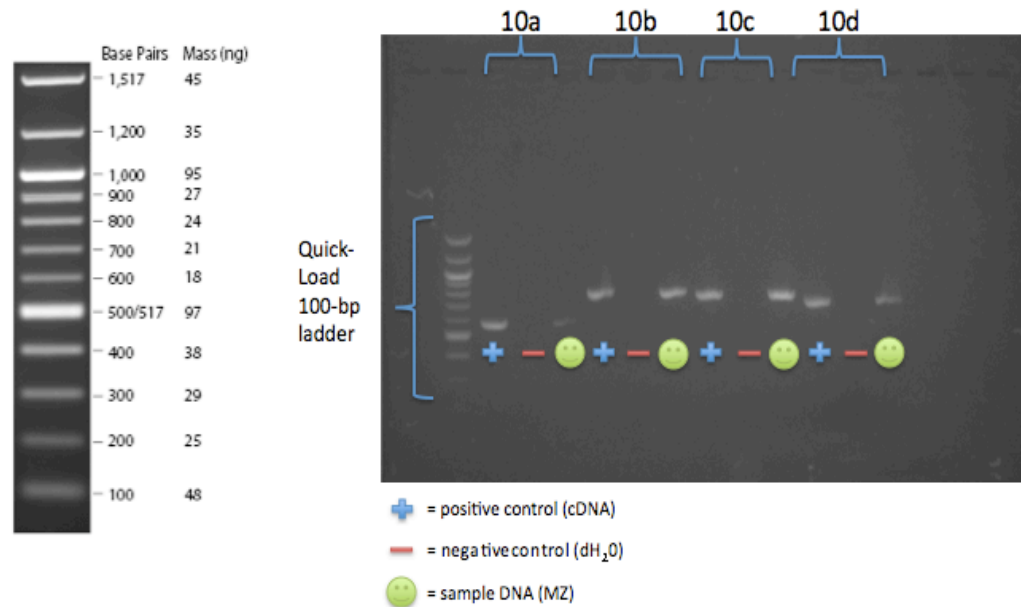


Figure 6 is a 1.8% agarose gel that is representative of the gels run for each of the samples that were amplified using PCR. The Quick-Load 100kb ladder was used to size each of the samples amplified.

After each product was confirmed via gel electrophoresis, they were sent to ElimBio for sequencing in both directions. The data collected from ElimBio was in the form of chromatograms. The chromatograms were analyzed for mutations.

7.2. Mutational Analysis

Mutational analysis of the ENAM gene showed a sequence variation in exon 7, at g.10602C>G. The mutation causes Pro to be replaced with Arg, which is indicative of an altered protein structure and function. Figure 7 shows the chromatograms for II:6, III:4, and II:7 and highlights the heterozygous mutation found in exon 7 for II:6 and III:4. The mother was homozygous for the wild type (normal).

Figure 7 Chromatogram of Exon 7 Mutation

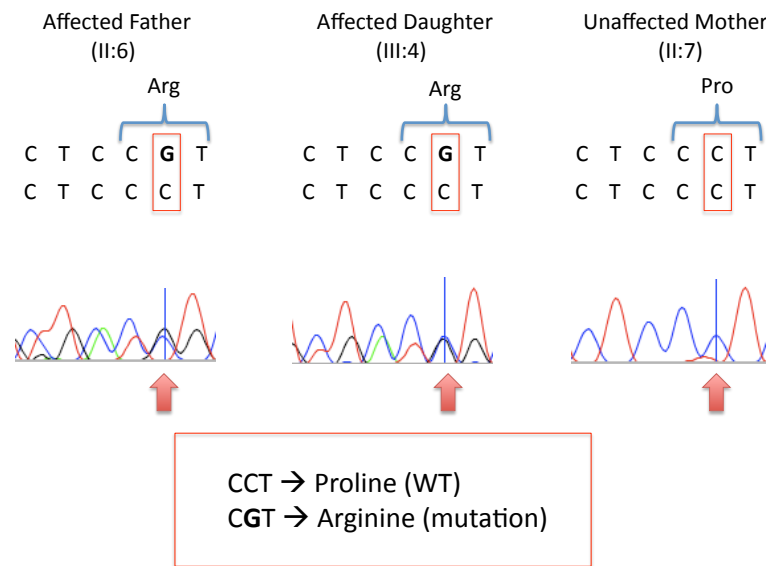


Figure 7 shows the chromatograms of the sequenced DNA at the same particular spot (10602) for III:4, her father II:6, and her mother II:7. The chromatograms show a heterozygous mutation (C>G) in III:4, and II:6, but the mother, II:7, remains homozygous for the normal sequence.

The missense mutation g.10602C>G codes for Arg instead of Pro. This particular position of the mutation in ENAM exon 7 represents an unchanged residue, which confirms the presence of strong functional constraints. The unchanged residues (black) as well as the conserved residues (shades of gray) are predicted to lead to enamel disorders when substituted by amino acids with different characteristics.²⁶ The proline residue is highly conserved through evolution. Homologues through crocodiles and lizards have a proline at this position. Every few residues in this region are a proline, which are seen in extended structures such as collagen and enamel pellicle proteins and are most likely associated with maturing enamel. As proline and arginine are two of the most different residues, this is likely the causative variant causing the family's AI.

Figure 8. Evolutionary Analysis of the Unchanged Residues in Exon 7

(a)



(b)

HUMAN ...PQQFPQYQMP...
 PIG ...PQFFPQYQMP...
 MOUSE ...PPQYPPYQMP...
 RAT ...PPQYPPYQMP...

Figure 8 shows (a) the unchanged Pro residue at g.10602 on Exon 7 as well as (b) the conservation between species at position 83.

Figure 9. Computational Modeling of Enamelin Protein Structures

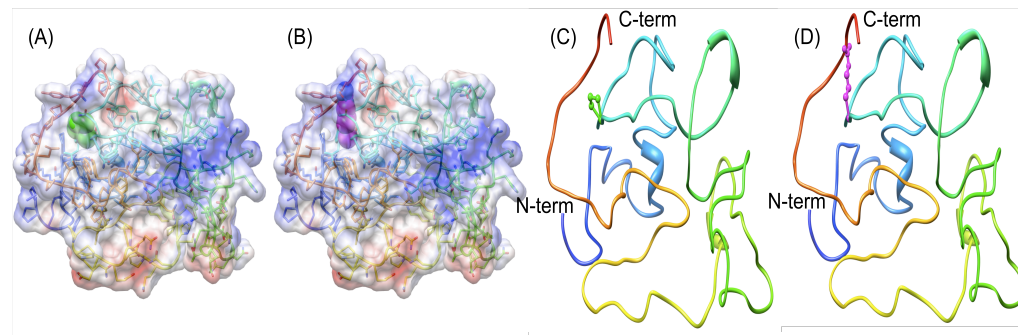


Figure 9 shows the computational modeling of enamel protein structures (excluding 39-residue signal peptide) as a result of P83(44)R mutation. Due to the lack of templates that reflect the known structures of proteins that share similar homology domains to those of enamel, “free modeling” was utilized to estimate wild-type (A, C) and mutated (B, D) enamel structures of the first 150(111) residues.

(A) and (B) The polypeptide backbone depicted as a ribbon, with the N-terminus in blue, and the progression to residue 150th(111th) in red. All side chains were shown as sticks, except position P83(44)R, which was shown as spheres. The Pro-83(44) atoms (spheres) are shown as green (A). The Arg-83(44) atoms were shown as pink, and blue for the nitrogens (B).

(C) and (D) With surface and side chains removed, model estimates showed that substitution of P83(44)R (red arrows in C and D) may inhibit proper protein folding due to the position of longer R’s side-chain in the mutant, altering enamel function.

Due to the results, which indicate this enamel missense mutation to be the causative entity, we did not deem it necessary to go the next step and create a transgenic mouse model. Even without a transgenic mouse model, we believe the results are strong enough to support our conclusion.

8. **Discussion**

8.1. The Role of the Dentist in Diagnosing and Treating AI

The family involved in this research study was pleased with the outcome of treatment and appreciated having the knowledge that the AI is in fact a genetic condition, is most likely autosomal, and is of a dominant inheritance pattern. Having this knowledge enables our patient to understand the risks of passing this trait on to her offspring. Because we know exactly where the mutation is, she could even opt for genetic screening in order to prepare for her child's possible AI condition.

In this study, we were able to utilize the laboratory setting for the purpose of purifying DNA from saliva, performing gel electrophoresis, and running PCR, all of which are basic lab techniques. The sequencing was outsourced and the initial candidate gene was chosen after an extensive literature review. Unfortunately, at this time, without laboratory skills and the resources of a university laboratory, a clinician is unable to make a definitive diagnosis for a patient when AI is suspected. However, a contemporary algorithm that clinicians and researchers alike can apply to all patients with AI is past due.

8.2. Photo Database of Previously Published AI Mutations

Enamel defects in AI are highly variable and range from deficiencies in enamel formation to defects in mineral and protein content. Even within the same genetic mutation, there can be great variability of the AI phenotype. For example, a brother and sister with the exact same genetic mutation causing AI may exhibit a very dissimilar phenotypic appearance. The variability in phenotype makes the

diagnosis of AI extremely confusing and difficult, especially when using the outdated AI classification systems. It is much more efficient to diagnose AI starting with familial inheritance pattern and using clinical enamel characteristics as a way to describe the condition and not solely to diagnose the condition.

The photo database is a compilation of all of the previously published mutations found to cause AI. It is clear that aside from some major generalizations, there are no obvious correlations between the AI causing mutation and the phenotype (see Appendix).

The definitions of enamel phenotype, however, are still relevant. The three main types of AI were defined previously and are correlated with defects in the stages of enamel synthesis. Hypoplastic (thin) enamel results from secretory stage pathologies. During the maturation stage, the enamel layer hardens by thickening and widening the crystals that were deposited during the secretory stage. In hypoplastic enamel, there is a defect in the enamel matrix caused by interference in ameloblast function. The enamel is typically thin and often has pitting due to apposition defects seen localized or generalized. Radiographically, the enamel is more radiopaque than the dentin. In the hypocalcified type, the enamel is of normal thickness but the mineralization process of the enamel matrix is defective. It tends to be the most severe form due to pathology starting in the secretory stage and continuing through maturation stage. Soft enamel is a result and radiographically, the enamel is less radiopaque than the dentin. In hypomature enamel, the defect is in the growth of the enamel crystals during the maturation phase. Proteins are not completely removed, which leads to a normal

enamel thickness lacking hardness. Radiographically, the radio opacity of the enamel is similar to that of the dentin.

8.3. Novel Algorithm for Clinicians

The proposed algorithm (Figure 10) starts with an inherited enamel defect and leads to the most likely candidate gene for mutational screening. The goal of this algorithm is to propose a user-friendly, step-by-step diagram, enabling clinicians to increase their understanding of the genetic etiologies of AI and choose the most likely candidate gene.

There are three key components, which are crucial to the design of the algorithm: the presence of an enamel defect, an inheritance pattern, and candidate genes for genetic analysis. This novel approach to AI diagnosis focuses primarily on familial inheritance pattern. Phenotype shall only be used to prioritize candidate genes, as there is a lack of close correlation between AI phenotype and molecular defect.

Figure 10. Algorithm using candidate-gene-based mutational analysis

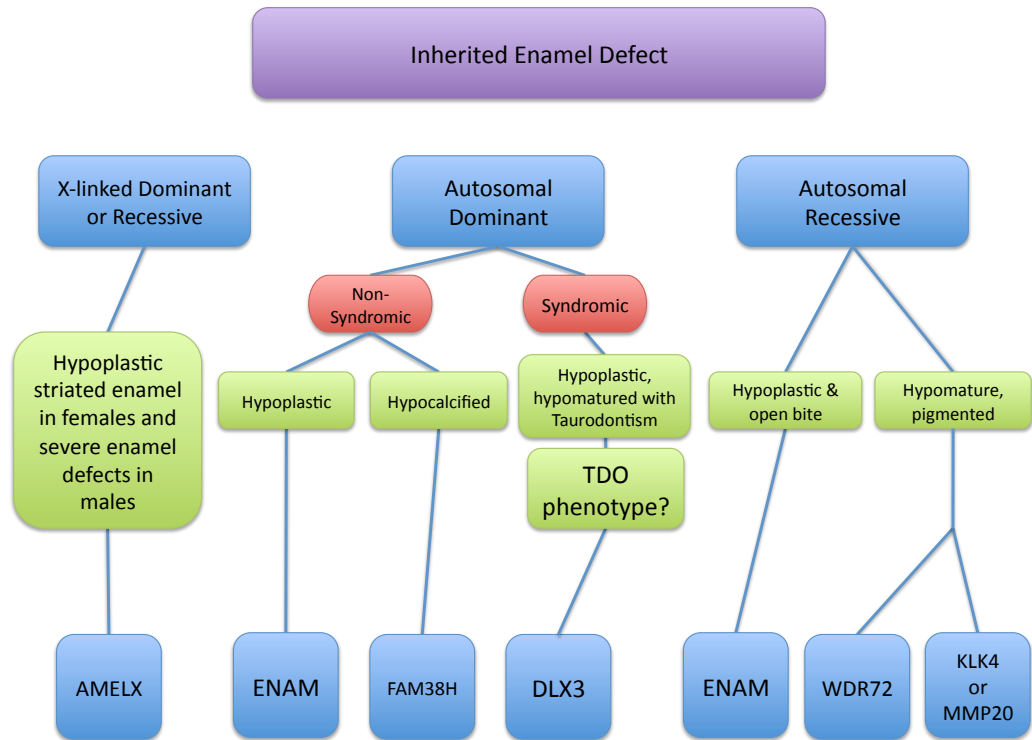


Figure 10 depicts the novel algorithm created for clinicians to diagnose AI based on a candidate gene based approach and without relying on confusing clinical phenotypes.

8.4. Applying the Algorithm to the Family Studied

Using the detailed steps described in the Methods section, as well as conducting an extensive and arduous literature review to choose the candidate gene, we were able to find the mutation-causing variant in enamelin.

Unfortunately, this process is not feasible for the private practitioner or public health dentist. The algorithm was created to simplify this process without

compromising a scientifically sound result. A clinician can collect saliva in the clinical setting and using the algorithm, can choose the most likely candidate gene(s). The laboratory steps can easily be outsourced and data can be analyzed so that the clinician can report results directly to the patient.

In the case of the research family, the saliva was easily collected in the dental clinic using the Oragene kits. A family inheritance diagram was collected and recorded. The inheritance pattern is undeniably dominant but whether it was autosomal or X-linked could not be discerned. As the patient and her parents are healthy individuals, the “syndromic” pathway can be ruled out. This leads us to the only option of phenotype, hypoplastic, which fit the description of the patient’s enamel. Continuing through the algorithm, the two candidate genes that result are AMELX and ENAM. AMELX has only been found in 5% of published AI mutations, so ENAM was chosen as the *most* likely candidate gene. Fortunately, the causative variant was found in ENAM, but if the data had come back “normal,” AMELX would have been the next most likely candidate gene to analyze.

The ability for practitioners to have access to a simple AI algorithm enables them to choose the most likely candidate gene(s) for their patients. The laboratory work and analysis of results can be outsourced and the mutated gene can be reported back to the patient.

9. **Conclusion**

The study showed the possibility of collecting saliva in the clinical setting and successfully diagnosing an inherited tooth defect. The notion was that salivary DNA could be purified and a candidate gene chosen for the purpose of diagnosing a genetic condition. The results of this study show the possibility of AI diagnosis in the clinical setting. The incorporation of the AI algorithm enables the clinician to choose the most likely candidate gene, thus minimizing the time and effort necessary to diagnose the condition.

The creation of the AI photo database was a compilation of previously published mutations causing AI. The general assessment of the photos and their respective mutations was that clinical phenotype and genetic diagnosis show considerable heterogeneity. The dated AI classification system from Witkop no longer holds up in the modern world where advancements in genetic research have changed the way we think about AI. The AI algorithm aims to be the stepping-stone to bringing mutational analysis into mainstream dentistry.

AI not only affects the teeth, but also the patient's oral hygiene, comfort level, and overall quality of life. The lifetime cost of restoring a patient's affected dentition is in the tens of thousands. The hope is that by obtaining a patient's genetic diagnosis, it will allow them to qualify for coverage and reduce the financial burden that inevitably comes with the disease.

This study proposes a paradigm shift in the diagnosis of AI and aims to encourage dentists and dental specialists to diagnose and treat patients with AI. The more prevalent the diagnoses, the more widely it will be known that AI is a genetic condition and not

solely the result of poor oral hygiene or dental negligence. As the advances in mutational genetics continue to advance, there will inevitably be even more changes to the way we diagnose, hopefully resulting in an even simpler process. In the meantime, keeping up with the current literature and diagnosing AI using the algorithm proposed in this study shall be a substantial upgrade from the classification system of the 1970s.

Based on this study's results, the following conclusions can be made:

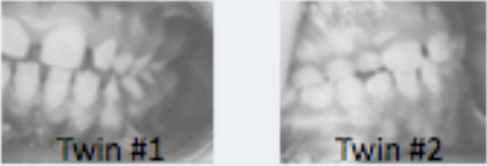

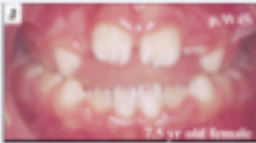


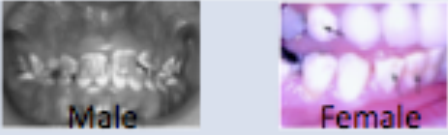
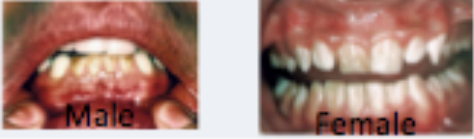
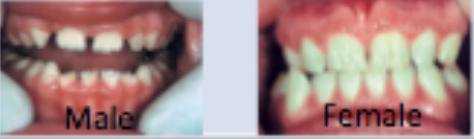
1. Saliva collection in the clinical setting can be used to extract a patient's DNA.
2. DNA from saliva can be used in the diagnosis of an inherited tooth related defects.
3. Likely candidate genes can be chosen by following the steps in the AI algorithm.
4. AI phenotype and genetic mutation often show wide heterogeneity.
5. Diagnosing AI using the candidate gene method shall be today's standard of clinical care.

10. **Acknowledgements**


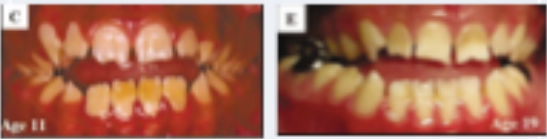

Research supported by the UCSF Start up fund to Dr. Thuan Le. I would also like to express my gratitude to the few, special colleagues who were invaluable to the completion and success of this project: Dr. Thuan Le, Dr. Pam Den Besten, Dr. Wu Li, Kaitlin Katsura, Dr. Jeremy Horst, the members of the Den Besten Craniofacial & Mesenchymal Biology laboratory, and the family upon whose genetic condition this study was based.

11. **Appendix: Photo Databank of Published AI Mutations**


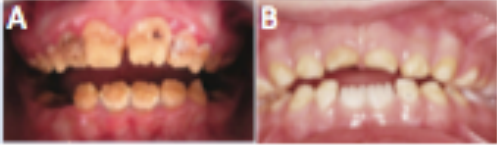





1. AMELX X-linked mutations^{27, 28-32}

AMELX X-linked		
Mutation	Clinical photo	Description
c.541delC; p.L181fsX187		Hypoplastic
c.2T→C; p.M1Tt		Hypoplastic
c.11G→C; p.W4S		Hypoplastic
c.152C→G; p.P52R		Hypoplastic
c.420delC; p.Y141fsx187		Hypoplastic
c.208C→A; p.P70T		Hypomature (?)
c.230A→VT; p.H77L		Hypoplastic
c.541delC; p.L181fsX187		Hypoplastic


2. ENAM Autosomal Dominant and Autosomal Recessive Mutations^{15, 19, 23, 25, 33-35}

ENAM AD and AR*		
Mutation	Clinical Photo	Description
c.157A→T; p.K53X		Hypoplastic
c.817G→T; p.R179M		Hypoplastic
c.534+1G→A; p.A158_Q178del		Hypoplastic
c.1020_1021insAGTCA		Hypoplastic*
c.211-2A→C; p.M71_Q157del		Hypoplastic
c.2991delT; p.L998fsX1062		Hypoplastic
c.1258_1259insAG; p.P422fsX448		Hypoplastic*

3. FAM83H Autosomal Dominant Mutations^{20, 36-40}

FAM83H AD		
Mutation	Clinical Photo	Description
c.1374C→A; p.Y458X		Hypocalcified
A. c.1192C→T; Q398X B. c.1330C→T; p.Q444X		Hypocalcified
c.1366C→T; p.Q456X		Hypocalcified
c.1354C→T; p.Q452X		Hypocalcified
A. c.1408C→T; p.Q470X B. c.1872_1873delCC; p.L625fsX703 C. c.2080G→T; p.E694X		Hypocalcified
c.1192C→T; Q398X		Hypocalcified
A. c.1243G→T; p.E415X B. c.891T→A; p.Y297X C. c.1380G→A; p.W460X D. c.2029C→T; p.Q677X		Hypocalcified



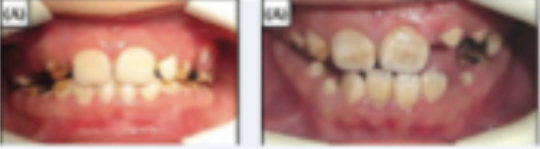

4. WDR72 Autosomal Dominant Mutations¹³

WDR72 AR		
Mutation	Clinical Photo	Description
<p>c.2348C→G; p.S783X (photos A, B, C)</p> <p>c.2857delA;p.S953VfsX20 (no photos)</p> <p>c.2934G→A; p.W978X (no photos)</p>	 <p>Three clinical photographs (A, B, C) showing hypomature teeth. Photo A is a frontal view of the upper teeth, photo B is a frontal view of the lower teeth, and photo C is a lateral view of the teeth. All photos show yellowish discoloration and irregular shapes of the teeth, characteristic of hypomaturity.</p>	Hypomature

5. KLK4 Autosomal Recessive Mutations⁴¹

KLK4 AR		
Mutation	Clinical Photo	Description
c.458G→A; p.W153X	 <p>A clinical photograph showing hypomature teeth with yellowish discoloration and irregular shapes, characteristic of hypomaturity.</p>	Hypomature

6. MMP20 Autosomal Recessive Mutations⁴²⁻⁴⁵

MMP20 AR		
Mutation	Clinical Photo	Description
c.678T→A; p.H226Q		Hypomature
c.102G→A; p.W34X		Hypomature
c.910G→A; p.A304T		Hypomature
c.954-2A→T; p.I319X or p.I319fs338X		Hypomature

12. References

1. Crawford PJ, Aldred M, Bloch-Zupan A. Amelogenesis imperfecta. *Orphanet J Rare Dis* 2007;2:17.
2. Hu JC, Chun YH, Al Hazzazzi T, Simmer JP. Enamel formation and amelogenesis imperfecta. *Cells Tissues Organs* 2007;186(1):78-85.
3. Fincham AG, Moradian-Oldak J, Simmer JP. The structural biology of the developing dental enamel matrix. *J Struct Biol* 1999;126(3):270-99.
4. Wright J. *Developmental Defects of the Teeth*. Chapel Hill, NC; 2009.
5. Wright JT. The molecular etiologies and associated phenotypes of amelogenesis imperfecta. *Am J Med Genet A* 2006;140(23):2547-55.
6. Urzua B, Ortega-Pinto A, Morales-Bozo I, Rojas-Alcayaga G, Cifuentes V. Defining a new candidate gene for amelogenesis imperfecta: from molecular genetics to biochemistry. *Biochem Genet* 2011;49(1-2):104-21.
7. Deutsch D, Palmon A, Dafni L, Catalano-Sherman J, Young MF, Fisher LW. The enamelin (tuftelin) gene. *Int J Dev Biol* 1995;39(1):135-43.
8. Deutsch D, Leiser Y, Shay B, Fermon E, Taylor A, Rosenfeld E, et al. The human tuftelin gene and the expression of tuftelin in mineralizing and nonmineralizing tissues. *Connect Tissue Res* 2002;43(2-3):425-34.
9. Gao Y, Wang W, Sun Y, Zhang J, Li D, Wei Y, et al. Distribution of amelotin in mouse tooth development. *Anat Rec (Hoboken)* 2010;293(1):135-40.
10. Kim JW, Simmer JP, Lin BP, Seymen F, Bartlett JD, Hu JC. Mutational analysis of candidate genes in 24 amelogenesis imperfecta families. *Eur J Oral Sci* 2006;114 Suppl 1:3-12; discussion 39-41, 379.
11. Lu Y, Papagerakis P, Yamakoshi Y, Hu JC, Bartlett JD, Simmer JP. Functions of KLK4 and MMP-20 in dental enamel formation. *Biol Chem* 2008;389(6):695-700.
12. Stephanopoulos G, Garefalaki ME, Lyroudia K. Genes and related proteins involved in amelogenesis imperfecta. *J Dent Res* 2005;84(12):1117-26.
13. El-Sayed W, Parry DA, Shore RC, Ahmed M, Jafri H, Rashid Y, et al. Mutations in the beta propeller WDR72 cause autosomal-recessive hypomaturation amelogenesis imperfecta. *Am J Hum Genet* 2009;85(5):699-705.
14. Hu JC, Yamakoshi Y. Enamelin and autosomal-dominant amelogenesis imperfecta. *Crit Rev Oral Biol Med* 2003;14(6):387-98.
15. Kim JW, Seymen F, Lin BP, Kiziltan B, Gencay K, Simmer JP, et al. ENAM mutations in autosomal-dominant amelogenesis imperfecta. *J Dent Res* 2005;84(3):278-82.
16. Rao S, Witkop CJ, Jr. Inherited defects in tooth structure. *Birth Defects Orig Artic Ser* 1971;7(7):153-84.
17. Aldred MJ, Savarirayan R, Crawford PJ. Amelogenesis imperfecta: a classification and catalogue for the 21st century. *Oral Dis* 2003;9(1):19-23.
18. Aldred MJ, Hall RK, Kilpatrick N, Bankier A, Savarirayan R, Lamande SR, et al. Molecular analysis for genetic counselling in amelogenesis imperfecta. *Oral Dis* 2002;8(5):249-53.
19. Kang HY, Seymen F, Lee SK, Yildirim M, Tuna EB, Patir A, et al. Candidate gene strategy reveals ENAM mutations. *J Dent Res* 2009;88(3):266-9.

20. Kim JW, Lee SK, Lee ZH, Park JC, Lee KE, Lee MH, et al. FAM83H mutations in families with autosomal-dominant hypocalcified amelogenesis imperfecta. *Am J Hum Genet* 2008;82(2):489-94.
21. Hart TC, Bowden DW, Bolyard J, Kula K, Hall K, Wright JT. Genetic linkage of the tricho-dento-osseous syndrome to chromosome 17q21. *Hum Mol Genet* 1997;6(13):2279-84.
22. Bailleul-Forestier I, Molla M, Verloes A, Berdal A. The genetic basis of inherited anomalies of the teeth. Part 1: clinical and molecular aspects of non-syndromic dental disorders. *Eur J Med Genet* 2008;51(4):273-91.
23. Rajpar MH, Harley K, Laing C, Davies RM, Dixon MJ. Mutation of the gene encoding the enamel-specific protein, enamelin, causes autosomal-dominant amelogenesis imperfecta. *Hum Mol Genet* 2001;10(16):1673-7.
24. Kida M, Ariga T, Shirakawa T, Oguchi H, Sakiyama Y. Autosomal-dominant hypoplastic form of amelogenesis imperfecta caused by an enamelin gene mutation at the exon-intron boundary. *J Dent Res* 2002;81(11):738-42.
25. Hart PS, Michalec MD, Seow WK, Hart TC, Wright JT. Identification of the enamelin (g.8344delG) mutation in a new kindred and presentation of a standardized ENAM nomenclature. *Arch Oral Biol* 2003;48(8):589-96.
26. Al-Hashimi N, Sire JY, Delgado S. Evolutionary analysis of mammalian enamelin, the largest enamel protein, supports a crucial role for the 32-kDa peptide and reveals selective adaptation in rodents and primates. *J Mol Evol* 2009;69(6):635-56.
27. Kindelan SA, Brook AH, Gangemi L, Lench N, Wong FS, Fearne J, et al. Detection of a novel mutation in X-linked amelogenesis imperfecta. *J Dent Res* 2000;79(12):1978-82.
28. Kim JW, Simmer JP, Hu YY, Lin BP, Boyd C, Wright JT, et al. Amelogenin p.M1T and p.W4S mutations underlying hypoplastic X-linked amelogenesis imperfecta. *J Dent Res* 2004;83(5):378-83.
29. Kida M, Sakiyama Y, Matsuda A, Takabayashi S, Ochi H, Sekiguchi H, et al. A novel missense mutation (p.P52R) in amelogenin gene causing X-linked amelogenesis imperfecta. *J Dent Res* 2007;86(1):69-72.
30. Greene SR, Yuan ZA, Wright JT, Amjad H, Abrams WR, Buchanan JA, et al. A new frameshift mutation encoding a truncated amelogenin leads to X-linked amelogenesis imperfecta. *Arch Oral Biol* 2002;47(3):211-7.
31. Hart S, Hart T, Gibson C, Wright JT. Mutational analysis of X-linked amelogenesis imperfecta in multiple families. *Arch Oral Biol* 2000;45(1):79-86.
32. Hart PS, Aldred MJ, Crawford PJ, Wright NJ, Hart TC, Wright JT. Amelogenesis imperfecta phenotype-genotype correlations with two amelogenin gene mutations. *Arch Oral Biol* 2002;47(4):261-5.
33. Mardh CK, Backman B, Holmgren G, Hu JC, Simmer JP, Forsman-Semb K. A nonsense mutation in the enamelin gene causes local hypoplastic autosomal dominant amelogenesis imperfecta (AIH2). *Hum Mol Genet* 2002;11(9):1069-74.
34. Gutierrez SJ, Chaves M, Torres DM, Briceno I. Identification of a novel mutation in the enamelin gene in a family with autosomal-dominant amelogenesis imperfecta. *Arch Oral Biol* 2007;52(5):503-6.

35. Ozdemir D, Hart PS, Firatli E, Aren G, Ryu OH, Hart TC. Phenotype of ENAM mutations is dosage-dependent. *J Dent Res* 2005;84(11):1036-41.
36. El-Sayed W, Shore RC, Parry DA, Inglehearn CF, Mighell AJ. Ultrastructural analyses of deciduous teeth affected by hypocalcified amelogenesis imperfecta from a family with a novel Y458X FAM83H nonsense mutation. *Cells Tissues Organs* 2010;191(3):235-9.
37. Hart PS, Becerik S, Cogulu D, Emingil G, Ozdemir-Ozenen D, Han ST, et al. Novel FAM83H mutations in Turkish families with autosomal dominant hypocalcified amelogenesis imperfecta. *Clin Genet* 2009;75(4):401-4.
38. Hyun HK, Lee SK, Lee KE, Kang HY, Kim EJ, Choung PH, et al. Identification of a novel FAM83H mutation and microhardness of an affected molar in autosomal dominant hypocalcified amelogenesis imperfecta. *Int Endod J* 2009;42(11):1039-43.
39. Wright JT, Frazier-Bowers S, Simmons D, Alexander K, Crawford P, Han ST, et al. Phenotypic variation in FAM83H-associated amelogenesis imperfecta. *J Dent Res* 2009;88(4):356-60.
40. Lee SK, Hu JC, Bartlett JD, Lee KE, Lin BP, Simmer JP, et al. Mutational spectrum of FAM83H: the C-terminal portion is required for tooth enamel calcification. *Hum Mutat* 2008;29(8):E95-9.
41. Hart PS, Hart TC, Michalec MD, Ryu OH, Simmons D, Hong S, et al. Mutation in kallikrein 4 causes autosomal recessive hypomaturation amelogenesis imperfecta. *J Med Genet* 2004;41(7):545-9.
42. Ozdemir D, Hart PS, Ryu OH, Choi SJ, Ozdemir-Karatas M, Firatli E, et al. MMP20 active-site mutation in hypomaturation amelogenesis imperfecta. *J Dent Res* 2005;84(11):1031-5.
43. Papagerakis P, Lin HK, Lee KY, Hu Y, Simmer JP, Bartlett JD, et al. Premature stop codon in MMP20 causing amelogenesis imperfecta. *J Dent Res* 2008;87(1):56-9.
44. Lee SK, Seymen F, Kang HY, Lee KE, Gencay K, Tuna B, et al. MMP20 hemopexin domain mutation in amelogenesis imperfecta. *J Dent Res* 2010;89(1):46-50.
45. Kim JW, Simmer JP, Hart TC, Hart PS, Ramaswami MD, Bartlett JD, et al. MMP-20 mutation in autosomal recessive pigmented hypomaturation amelogenesis imperfecta. *J Med Genet* 2005;42(3):271-5.

